THE JOURNAL OF PHYSICAL CHEMISTRY B

Article

pubs.acs.org/JPCB

Host–Guest Chemistry of Dendrimer–Cyclodextrin Conjugates: Selective Encapsulations of Guests within Dendrimer or Cyclodextrin Cavities Revealed by NOE NMR Techniques

Hui Wang,[†] Naimin Shao,[†] Shengnan Qiao,[†] and Yiyun Cheng*[,†,‡]

[†]Shanghai Key Laboratory of Regulatory Biology, School of Life Sciences, East China Normal University, Shanghai, 200241, P. R. China

[‡]Shanghai Key Laboratory of Magnetic Resonance, Department of Physics, East China Normal University, Shanghai, 200062, P. R. China

Supporting Information

ABSTRACT: In this study, G5 PAMAM dendrimer and α-, β-, γ-cyclodextrin (CD) conjugates were synthesized. Host–guest behaviors of the conjugates toward five guest molecules including sodium methotrexate (MTX), amantadine hydrochloride (ADH), sulfamethoxazole (SMZ), sodium deoxycholate (SDC), and sodium dodecyl sulfate (SDS) were analyzed by NOE NMR techniques. Among the five guest molecules, ADH only binds with β-CD in G5–β-CD, SDC shows higher priority to localize within the cavity of γ-CD in G5–γ-CD, while MTX exhibits selective encapsulation within the cavities of G5 dendrimer in G5–α-CD. SDS has high binding affinity with α-CD in G5–α-CD but forms a precipitate in the complex solution. SMZ shows simultaneous encapsulation within CDs (α-, β-, and γ-CD) or G5 in the presence of the three conjugates. The host behavior of G5–CD conjugates depends on CD cavity size, guest size, and hydrophobicity. The results obtained in this study are helpful in the optimization of dendrimer–CD conjugate-based drug delivery systems.

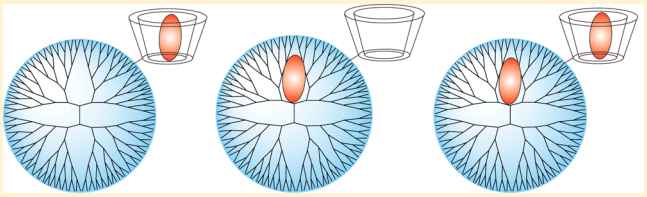

INTRODUCTION

Dendrimers, synthesized in an iterative sequence of reaction steps, are hyperbranched and reactive three-dimensional macromolecules, with all bonds emanating from a central core.[1−3] They have well-defined nanostructures with globular shapes, interior pockets, high degree of molecular uniformity and excellent monodispersity, and high density of surface functionalities.[3] The interior pockets of dendrimers can encapsulate drug molecules via noncovalent interactions such as electrostatic, hydrophobic, and hydrogen-bond interactions, while surface functionalities of dendrimers can be modified with drug molecules by covalent strategies.[4,5] There are numerous reports on dendrimer-based drug delivery systems, including the use of dendrimers to improve drug solubility and bioavailability, to achieve sustained drug release, to deliver genetic drugs into cell nucleus, and as scaffolds for the design of targeted drug delivery systems.[6−10] Among the frequently used dendrimers in biomedical applications, poly(amidoamine) (PAMAM) dendrimers which were first synthesized by Tomalia in 1985 are the most investigated, in-depth characterized, and now commercially available ones.[3,11]

PAMAM dendrimers with different surface functionalities have the ability to encapsulate a list of guest molecules including phenylbutazone, phenobarbital, mycophenolic acid, sulfamethoxazole (SMZ), sodium deoxycholate (SDC), and sodium dodecyl sulfate (SDS).[12−15] Recently, our group found that PAMAM dendrimers can even encapsulate some large guest molecules such as dexamethasone 21-phosphate, Congo red, and indocyanine green with molecular weights up to 775 Da.[16,17] However, limited drugs are beneficial from the PAMAM dendrimer-based drug delivery systems. Our previous studies have found that drug molecules such as amantadine hydrochloride (ADH), propranolol hydrochloride, primidone, and trimethoprim (TMP) failed to form inclusion complexes with PAMAM dendrimers.[18,19] Among the library of drug candidates, only a small percent of drugs can form stable complexes with PAMAM dendrimers. Therefore, there is an urgent need to design new drug carriers based on PAMAM dendrimers to make more drugs benefit from the dendrimer technology.

Cyclodextrins (CDs) are cyclic oligosaccharides of six to eight glucopyranose units linked by R-1,4 linkages, which are called α-, β-, and γ-CD, respectively.[20] Their hydrophilic exterior makes CDs water-soluble, while their hydrophobic internal cavities can encapsulate a wide range of size-matched guest molecules, especially those hydrophobic ones.[21,22] During the past decades, numerous CD derivatives were synthesized to improve their complexation properties and to make them suitable for biomedical applications.[23] However, guest molecules complexed with CDs and their derivatives are often at low

Received: June 26, 2012
Revised: August 15, 2012
Published: August 30, 2012

dx.doi.org/10.1021/jp3062916 | J. Phys. Chem. B 2012, 116, 11217−11224

molar ratios (1:1 or 1:2 for α-, β-, and γ-CDs). Hence, CDs and their derivatives showed much lower ability in the solubilization of hydrophobic drugs than dendrimers.[24]

Dendrimer−CD conjugates may combine the advantages of dendrimers and cyclodextrins.[25,26] CDs modified on dendrimer surface can improve the aqueous stability and biocompatibility of cationic PAMAM dendrimers which were reported with non-negligible cytotoxicity.[7] Also, CDs can sufficiently bind cholesterol, cholic acids, and other lipid molecules located on cell membrane, thus improving the cellular uptake of dendrimer−CD conjugates.[27] Furthermore, dendrimer−CD conjugates can extend the range of drug candidates loaded by dendrimer and CDs. Moreover, it is well-known that combination therapy with more than one therapeutic agent can not only improve the therapeutic efficiency but also decrease the drug-resistant effect and the intolerable side effect.[13] The dendrimer−CD conjugates can load different kinds of drugs, making it possible for combination therapy. For example, antibacterial agents SMZ and TMP are usually given together to patients. SMZ can form inclusion complex with PAMAM dendrimer while TMP can be encapsulated within the CD cavities.[19,28] The dendrimer−CD conjugates provide a solution to the design of drug formulations for combination therapy. Up to now, dendrimer−CD conjugates were widely used as gene carriers in refs 25, 27, 29, and 30 but few reports were focused on the potential drug delivery applications.[31]

In the present study, generation 5 (G5) PAMAM dendrimers were conjugated with α-, β-, and γ-CDs by two synthetic strategies. The host−guest behaviors of the three synthesized conjugates toward five guest molecules were investigated by nuclear Overhauser enhancement (NOE) NMR techniques. To the best of our knowledge, this is the first report on the drug binding behaviors of dendrimer−CD conjugates. The goal of this study is to provide physicochemical insights into the design of drug formulations based on dendrimer−CD conjugates.

EXPERIMENTAL SECTION

Materials. G5 ethylenediamine (EDA)-cored and amine-terminated PAMAM dendrimer was purchased from Dendritech, Inc. (Midland, MI). The CDs including α-, β-, and γ-CD, dimethyl sulfoxide (DMSO), and sodium hydroxide were obtained from Aladdin Inc. (Shanghai, China). *N,N′*-Carbonyldiimidazole (CDI) and *p*-toluenesulfonyl chloride (TsCl) were purchased from Sigma−Aldrich (St. Louis, MO). ADH was purchased from Wuhan Yuancheng Technology Development Co., Ltd. (Wuhan, China). SDS, SDC, and methotrexate disodium (MTX) were obtained from Shanghai BBI Co., Ltd. (Shanghai, China). SMZ was obtained from Shouguang Fukang Pharmacy Factory (Shandong, China). Deuterium oxide (D_2O) was purchased from Beijing Chongxi High-Tech Incubator Co., Ltd. (Beijing, China). Acetonitrile and hydrochloric acid were purchased from Sinopharm Chemical Reagent Co. Ltd. (Shanghai, China). G5 PAMAM dendrimer was received in methanol solution, and the solvent was distilled to obtain the dendrimer in a white gel. All the other chemicals were used as received without further purification.

Synthesis of G5−CD Conjugates. Method I. β-CD (101.6 g, 0.09 mol) was added to a 1% sodium hydroxide aqueous solution to which an acetonitrile solution containing TsCl (17.1 g, 0.09 mol) was added dropwise at room temperature.[27,31] After 2 h, 1 M hydrochloric acid was added to the reaction mixture to adjust the pH value of the solution to 6.20. After that the solution was stored at 4 °C overnight and the yield, a white precipitate, was harvested. The crude product was purified by recrystallization from water and washed several times with acetonitrile. The product was characterized by ^{1}H NMR (699.804 MHz, DMSO-d_6): δ 2.50 ppm (TsCl-CH_3), 3.30−3.70 ppm ($H_{2,4}$), 4.10−4.50 ppm ($H_{5,6}$), 4.84 ppm (H_3), 5.71 ppm (H_1), 7.40 ppm (TsCl-Ar), 7.80 ppm (TsCl-Ar).

G5 PAMAM dendrimer (51.5 mg, 1.8 μmol) and different amounts of monotosylated β-CD were dissolved in 6 mL of DMSO. The reaction mixture was stirred for 5 days at 60 °C. The product was purified by extensive dialysis (MWCO is 8000−14 000 Da) against DMSO and double-distilled water. The synthesized G5−β-CD was obtained as a yellow powder after lyophilization and stored at 4 °C before further use. ^{1}H NMR (D_2O): H_a, 2.36 ppm (−NCH_2CH_2CONH−); H_b, 2.59 ppm (−$CONHCH_2CH_2N$−); H_c, 2.78 ppm (−NCH_2CH_2-CONH−); $H_{b'}$, 3.05 ppm (−$CONHCH_2CH_2$NH−O−β-CD); H_d, 3.26 ppm (−$CONHCH_2CH_2N$−); $H_{d'}$, 3.43 ppm (−$CONHCH_2CH_2$NH−O−β-CD); $H_{2,4}$, 3.60−3.63 ppm; $H_{5,6}$, 3.78−3.81 ppm; H_2, 3.92 ppm; H_1, 5.00 ppm, 5.36 ppm.

Method II. To a DMSO solution containing β-CD (258.8 mg, 0.23 mmol) and CDI (37.2 mg, 0.23 mmol), G5 PAMAM dendrimer (51.2 mg, 1.8 μmol) solution was added dropwise.[20,32] The reaction mixture was stirred for 60 h at room temperature. The product was purified by extensive dialysis (MWCO is 8000−14 000 Da) against double-distilled water. The yielded G5−β-CD was obtained in a white powder after lyophilization and stored at 4 °C before further use. G5−α-CD and G5−γ-CD conjugates were prepared using the same strategy as described above.

All of the conjugates were characterized by ^{1}H NMR spectroscopy. ^{1}H NMR for G5−β-CD in D_2O: $H_{a,a'}$, 2.40 ppm, 2.43 ppm (−NCH_2CH_2CONH−); H_b, 2.60 ppm (−$CONHCH_2CH_2N$−); H_c, 2.80 ppm (−NCH_2CH_2CONH−); $H_{b'}$, 2.94 ppm (−$CONHCH_2CH_2$NH−O−β-CD); H_d, 3.28 ppm (−$CONHCH_2CH_2N$−); $H_{d'}$, 3.37 ppm (−$CONHCH_2CH_2$-NH−O−β-CD); H_4, 3.56 ppm; H_2, 3.62 ppm; $H_{5,6}$ 3.84 ppm; H_3, 3.92 ppm; H_1, 5.04 ppm.

G5−α-CD: $H_{a,a'}$ 2.40 ppm, 2.44 ppm (−NCH_2CH_2-CONH−); H_b, 2.61 ppm (−$CONHCH_2CH_2N$−); H_c, 2.80 ppm (−NCH_2CH_2CONH−); $H_{b'}$, 2.95 ppm (−$CONHCH_2CH_2$NH−O−α-CD); H_d, 3.28 ppm (−$CONHCH_2CH_2N$−); $H_{d'}$, 3.38 ppm (−$CONHCH_2CH_2$NH−O−α-CD); H_4, 3.56 ppm; H_2, 3.60 ppm; $H_{5,6}$, 3.82 ppm; H_3, 3.94 ppm; H_1, 5.03 ppm.

G5−γ-CD: $H_{a,a'}$ 2.39 ppm, 2.43 ppm (−NCH_2CH_2-CONH−); H_b, 2.60 ppm (−$CONHCH_2CH_2N$−); H_c, 2.80 ppm (−NCH_2CH_2CONH−); $H_{b'}$, 2.95 ppm (−$CONHCH_2$-CH_2NH−O−γ-CD); H_d, 3.27 ppm (−$CONHCH_2CH_2N$−); $H_{d'}$, 3.38 ppm (−$CONHCH_2CH_2$NH−O−γ-CD); H_4, 3.55 ppm; H_2, 3.63 ppm; $H_{3,5,6}$ 3.84 ppm; H_1, 5.07 ppm.

NMR Analysis. ^{1}H NMR experiments for G5−CDs conjugates and drug complexes in D_2O were conducted on a Varian 699.804 MHz NMR spectrometer at 298.2 ± 0.1 K. Generally, 1 mg of G5−CD conjugates or G5−CDs/drug complexes was dissolved in 500 μL of D_2O solution. The solutions were sonicated for 2 h before NMR studies.

COSY spectra of the G5−CD conjugates were obtained by the standard pulse program at Varian 699.804 MHz NMR spectrometer, with 1024 × 256 data points. The relaxation delay was 1 s. Eight scans were averaged. A sine-bell-squared window function and zero filling were applied to both dimensions.

Scheme 1. Synthesis Routes of G5−CDs Conjugates by Method I (a) and Method II (b)

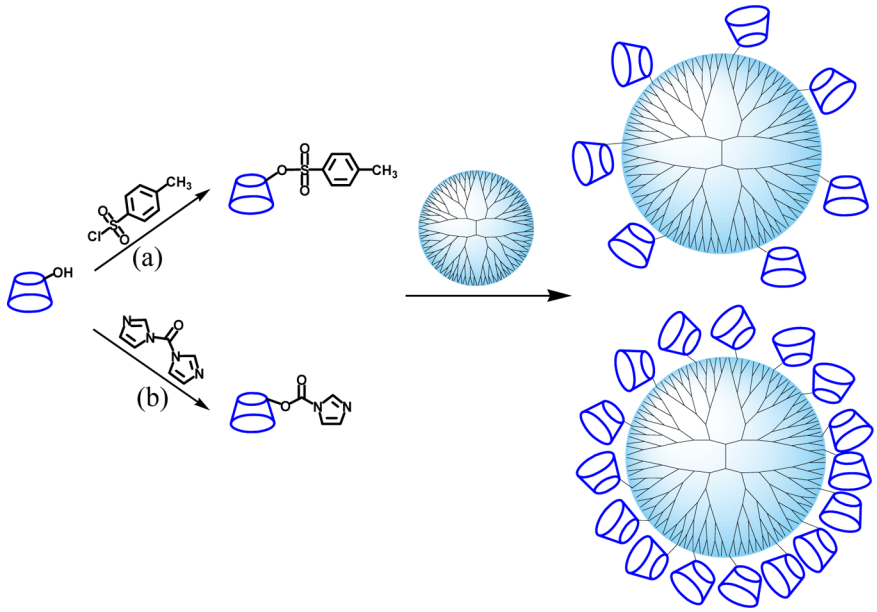

The ^{1}H−^{1}H 2D-NOESY experiments for G5−CD/guest complexes (G5−α-CD, G5−β-CD, and G5−γ-CD with ADH, SMZ, SDS, MTX, and SDC) were conducted on the same Varian 699.804 MHz NMR spectrometer using standard pulse sequences. One second relaxation delay, 146.63 ms acquisition time, a 6.5 μs 90° pulse width, and a 300 ms mixing time were chosen. Thirty-two transients were averaged for 1024 × 256 complex points. All the data were processed with NMRpipe software on a Linux workstation.

RESULTS AND DISCUSSION

Synthesis and Characterization of G5−CD Conjugates. G5−α-CD, G5−β-CD, and G5−γ-CD conjugates were synthesized according to Scheme 1. In the first strategy (Scheme 1a), β-CD was activated by TsCl and the monotosylated CDs were reacted with dendrimer surface according to refs 27 and 31. In the second strategy (Scheme 1b), the α-, β-, and γ-CDs were activated by CDI and followed by their conjugation to G5 dendrimer surface. The synthesized G5−CD conjugates by the two strategies were identified by ^{1}H NMR spectra. As shown in Figure 1, all the G5−CD conjugates show characteristic peaks for both dendrimers and CDs (H_a−H_d for G5 dendrimer interior scaffold methylene protons, $H_{b'}$ and $H_{d'}$ for G5 dendrimer outmost layer methylene protons, H_1−H_6 for CD protons). With the help of COSY spectrum in Figure 2 and Figure S1 in the Supporting Information, the proton resonance assignments in G5−CD conjugates were simplified and are shown in Figure 1 and Scheme 2. The peaks of H_3, H_5, and H_6 for G5−γ-CD are overlapped with each other, while the peak H_3 is separated from peaks $H_{5,6}$ for G5−α-CD and G5−β-CD, which is due to the inherent properties of α-, β-, and γ-CDs. Besides the G5 dendrimer and CD proton resonances, G5−β-CD conjugates synthesized by the first strategy show additional resonances at 2.35, 7.32, and 7.65 ppm, which were assigned to the TsCl protons. The residual TsCl groups were bound to the amine surface of G5 dendrimer and are not easy to remove from the conjugates. In comparison, no residual peaks for CDI can be observed in the ^{1}H NMR spectra of G5−CD conjugates synthesized by the second strategy. By integrating the peak areas of CD protons (42, 49, and 56 methylene protons for each α-, β-, and γ-CD, respectively, Scheme 2) and G5 dendrimer protons (504

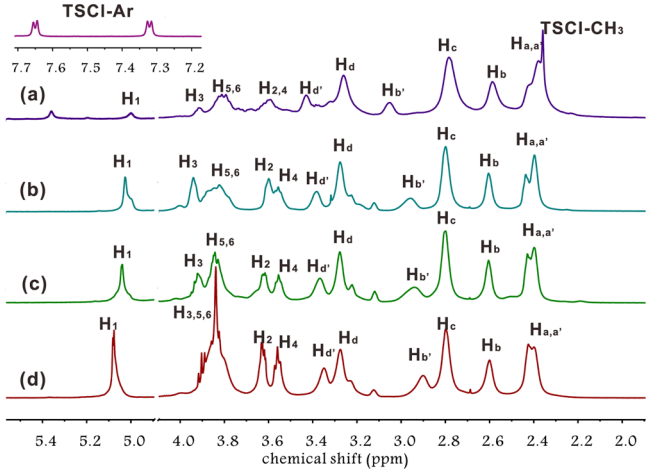

Figure 1. ^{1}H NMR spectra of the G5−CDs conjugates by the two synthetic routes: (a) G5−β-CD conjugate synthesized by method I; (b,c,d) G5−α-CD, G5−β-CD, and G5−γ-CD conjugates synthesized by method II, respectively.

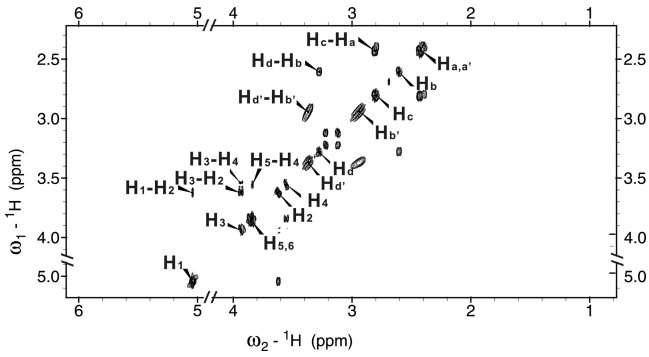

Figure 2. ^{1}H−^{1}H COSY spectrum of G5−β-CD synthesized by method II.

dx.doi.org/10.1021/jp3062916 | J. Phys. Chem. B 2012, 116, 11217−11224

Scheme 2. Chemical Structures of the Synthesized G5−CD Conjugates with Proton Labeling

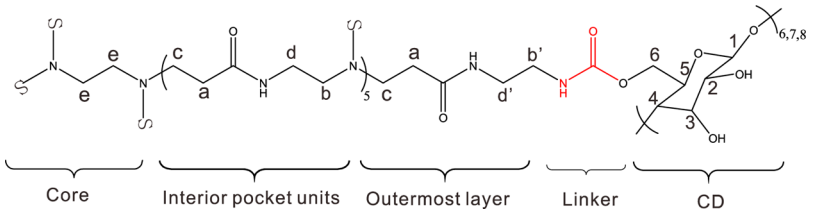

methylene protons for H_a, Scheme 2), the numbers of α-, β-, and γ-CD molecules conjugated on each G5 dendrimer synthesized by the second strategy are calculated to be 31.1, 36.0, and 32.5, respectively (Table 1). It is observed that the CD conjugation efficiency of the G5−CD conjugates by the second strategy is much higher than that by the first one. Therefore, the materials used in later NOE NMR analysis were synthesized by the second strategy.

Table 1. Characterization Data for the Synthesized G5−CD Conjugates by the Two Strategies

conjugates	conjugate method	CD/G5 feeding ratio	no. of CD conjugated	no. of TsCl or CDI
G5−α-CD	II	128:1	31.1	0
G5−β-CD	I	128:1	9.8	15
	I	64:1	7.4	7.2
	II	128:1	36.0	0
G5−γ-CD	II	128:1	32.5	0

Host−Guest Behavior of the Three G5−CD Conjugates. In order to evaluate the guest binding behavior of G5−CD conjugates, we prepared the complexes of G5−CD conjugates with five types of guest molecules including ADH, MTX, SMZ, SDS, and SDC (Scheme 3). Localizations of the guests within dendrimer interior pockets or CD cavity were analyzed by NOE NMR studies. NOESY techniques were proved to be an effective tool in the characterization of inclusion complexes.[12,33] They provide precise information on spatial distance between host and guest molecules.[34] Host and guest molecules in close spatial proximity relative to each other show NOE cross peaks in the corresponding region of the NOESY spectrum.[33] In the present study, ^{1}H−^{1}H NOESY experiments were carried out to characterize the inclusion complexes of G5−CD conjugates and the five guest molecules. Since 31.1, 36.0, and 32.5 CD molecules were conjugated on each G5 dendrimer for G5−α-CD, G5−β-CD, and G5−γ-CD, respectively, and each CD has one hydrophobic cavity for guest encapsulation, considering the possibility of sandwiched complexes of one guest with two CD molecules, the molar ratio of guest/G5−CD conjugate is kept constant at 16:1 in this study and this guest/carrier molar ratio can reveal the competitive binding behaviors of guest molecules to α-, β-, and γ-CDs and G5 PAMAM dendrimer.

Figure 3 and Figure S2 in the Supporting Information show the ^{1}H−^{1}H NOESY and ^{1}H NMR spectra of G5−α-CD, G5−β-CD, and G5−γ-CD with ADH, respectively. NOE cross peaks were observed between all ADH protons and β-CD protons (H_{1-6}/$H_{\alpha,\beta,\gamma}$) for the G5−β-CD/ADH complex, while no cross peak was observed between ADH and G5 dendrimer protons (H_{a-d}, Figure 3a, Scheme 2), suggesting that ADH molecules only bind with β-CD in the G5−β-CD conjugate. It is well-known that ADH has strong binding affinity with CD molecules since the adamantyl group in ADH is hydrophobic and its molecular size perfectly matches the cavities of CD molecules.[35] Therefore, adamantane and its derivatives were widely used in the design of CD-based molecular recognition

Scheme 3. Chemical Structures of the Five Selected Guest Molecules in the Present Study

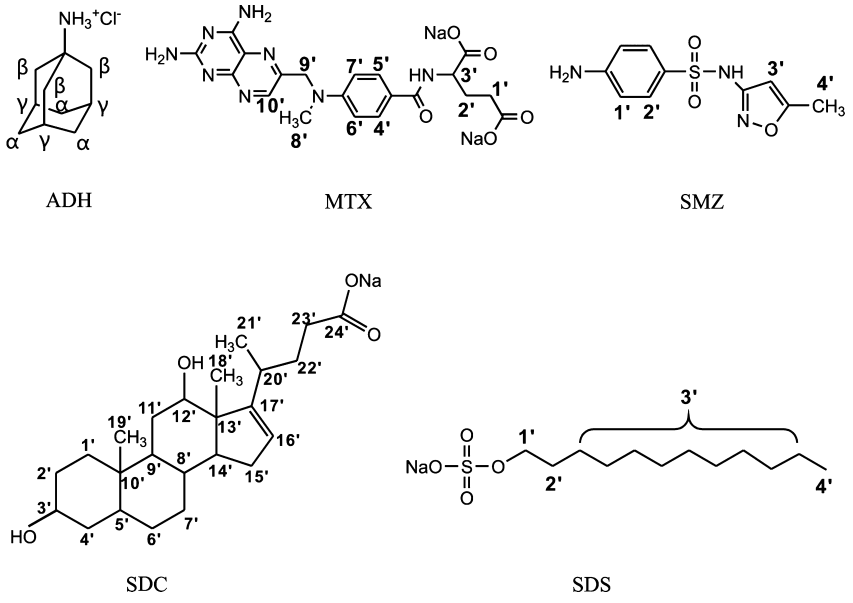

dx.doi.org/10.1021/jp3062916 | J. Phys. Chem. B 2012, 116, 11217−11224

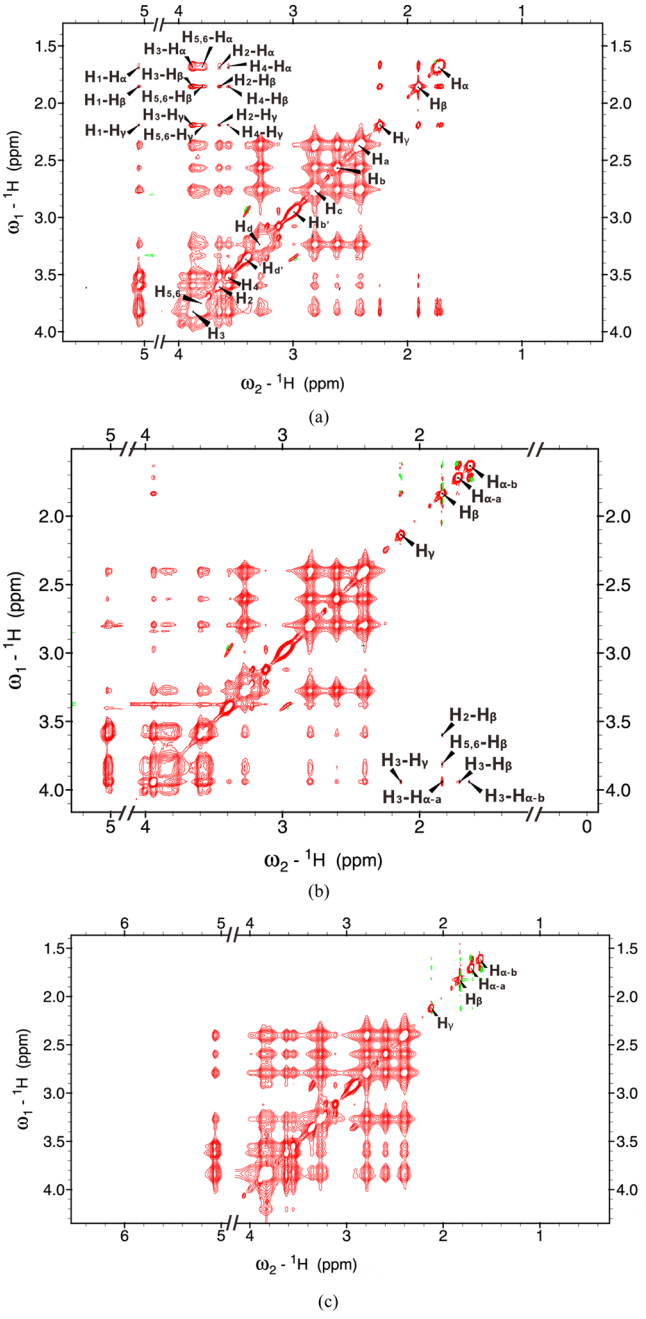

Figure 3. ^{1}H−^{1}H NOESY spectra of the ADH/G5−CDs complexes in D_2O: (a) ADH/G5−β-CD, (b) ADH/G5−α-CD, and (c) ADH/G5−γ-CD. The molar ratio of ADH and G5−CDs is 16.

devices, affinity biosensors, and supramolecular hydrogels.[36] In the CD molecular structure, H_3 and H_5 protons are located in the inner cavity of α-, β-, and γ-CD molecules. The stronger NOE cross peak between ADH protons ($H_{\alpha,\beta,\gamma}$) and β-CD inner cavity protons (H_3 and H_5) than that between $H_{\alpha,\beta,\gamma}$ and $H_{1,2,4}$ in Figure 3a confirmed that the adamantyl group region of ADH is encapsulated within β-CD cavity and that β-CD molecules conjugated on G5 dendrimer surface still have the ability to form inclusion complexes with guest molecules. Though the interior pockets of G5 dendrimer are relatively nonpolar, it failed to form inclusion complexes with ADH molecules, probably due to the small size and hydrophilic property of ADH molecules. The absence of ADH encapsulation within G5 dendrimer is in accordance with previous results on the NOESY spectrum of G4.5/ADH complexes.[18]

Similar results were obtained in the NOESY spectrum of G5−α-CD/ADH complex in Figure 3b. Weak cross peaks between ADH and α-CD protons (H_3/$H_{\alpha,\beta,\gamma}$, and $H_{2/5/6}$/H_β) and the absence of NOE interactions between G5 dendrimer and ADH protons are observed. The NOE peak intensity is in proportion to the number of equivalent protons and in inverse proportion to the distance between specific protons. Here, α-CD has a smaller cavity size than β-CD. The distance between ADH ($H_{\alpha,\beta,\gamma}$) and CD protons (H_{1-6}) is larger in the ADH/β-CD complex than in the ADH/α-CD complex. In this case, the weaker NOE cross peaks between ADH and α-CD in Figure 3b suggest the encapsulation of fewer ADH molecules within α-CD cavity as compared to the G5−β-CD/ADH complex. This is further confirmed by the much weaker intramolecular NOE interactions among H_α, H_β, and H_γ protons in comparison with that observed in Figure 3a. The orientation of ADH molecule within the α-CD cavity is the same as that within the β-CD cavity. However, no NOE interactions between ADH protons and γ-CD as well as G5 dendrimer protons are observed in Figure 3c, suggesting that no inclusion complex is formed between G5−γ-CD and ADH molecules. These results indicate that G5−β-CD conjugate is the best choice in the delivery of ADH molecules. The binding affinity of CD with guest molecule depends on guest size, CD cavity size, and hydrophobicity of the guest.[37] The adamantyl group in ADH is a spherical group with a diameter of 7 Å, and this size perfectly matches the cavity diameter of β-CD. The association equilibrium constants between adamantane derivatives and β-CD are reported to be as high as 10^5 M^{-1}.[35] Therefore, G5−β-CD shows stronger affinity to bind ADH molecules than the other two conjugates.

Figure 4a and Figure S3 in the Supporting Information show the NOESY spectra of the complexes of SDS with G5−γ-CD, G5−α-CD, and G5−β-CD. Strong NOE cross peaks between the inner pocket protons (H_3, H_5, and H_6) of β/γ-CD molecules and the aliphatic chain protons ($H_{3'}$) of SDS molecules are observed, suggesting the encapsulation of SDS molecules within the inner cavities of β- and γ-CD molecules in these complexes. In comparison, extremely weak NOE interactions between SDS protons and G5 dendrimer protons are observed in these NOESY spectra. Our previous studies found that SDS molecules are either bound on cationic dendrimer surface or encapsulated within dendrimer interior pockets. At SDS/G4 molar ratio of 8:1 to 16:1, SDS molecules mainly locate in the interior pockets of G4 PAMAM dendrimer and strong NOE cross peaks between dendrimer and SDS protons were observed.[38,39] Here, the SDS/G5−CD complexes at a molar ratio of 16:1 show extremely weak NOE cross peaks between SDS and G5 dendrimer but strong NOE interactions between SDS and CDs, indicating that SDS molecules have higher priority to bind with CD cavities rather than with G5 dendrimer in the conjugates. This is attributed to the more hydrophobic microenvironment of the CD cavity than that of the G5 interior pockets. Surprisingly, no NOE cross peak between SDS and G5 dendrimer as well as α-CD is observed in Figure S3a. This is because a white precipitate is formed after the addition of SDS molecules into G5−α-CD solution at a molar ratio of 16:1. As a result, the signal intensities of SDS protons in SDS/G5−α-CD are much lower than that in SDS/G5−β-CD and SDS/G5−γ-CD (Figure 4b). α-CD is reported to have strong binding affinity with long aliphatic acid and their

dx.doi.org/10.1021/jp3062916 | J. Phys. Chem. B 2012, 116, 11217−11224

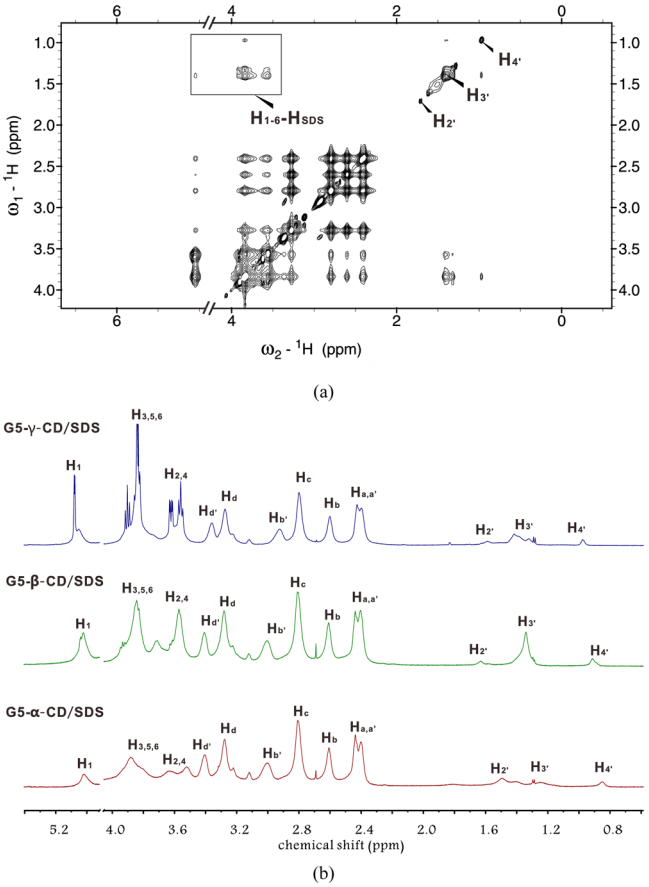

Figure 4. (a) ^{1}H−^{1}H NOESY spectrum of the SDS/G5−γ-CD complex in D_2O. (b) ^{1}H NMR spectra of G5−α-CD, G5−β-CD, and G5−γ-CD with SDS. The molar ratio of SDS and G5−β-CD is 16.

salts.[40] Among the three CDs, α-CD forms the most stable complexes with alkyltrimethylammonium bromides (C_{12} and C_{14}) and shows the highest equilibrium constants.[41] Due to the different cavity size of the three CDs, the stoichiometry of the CDs/alkyltrimethylammonium bromide complexes are calculated to be 2:1, 1:1, and 1:2 for α-, β-, and γ-CD, respectively.[41] The addition of SDS can lead to the displacement of aromatic compounds such as *p*-xylene from the α-CD cavity.[42] The strong binding affinity of SDS with α-CD cavities on the surface of G5 dendrimer results in a significant decrease in aqueous solubility of the formed SDS/α-CD complex, which well explains the formation of SDS/G5−α-CD precipitates.

The NOESY spectra of SDC/G5−CD complexes are shown in Figure 5 and Figure S4 in the Supporting Information. In the spectra of SDC/G5−γ-CD and SDC/G5−β-CD, strong NOE cross peaks are observed between β/γ-CD and SDC molecules and extremely weak NOE signals are observed between SDC and G5 dendrimer (Figure 5). Our previous NOE studies have demonstrated the formation of a stable SDC/G5 PAMAM inclusion complex in aqueous solution.[14] However, NOE results in this study revealed that SDC prefers to bind with β/γ-CD rather than with G5 PAMAM in the presence of G5−β/γ-CD conjugates. In comparison, medium cross peaks between SDC and G5/α-CD are observed in Figure S4a, suggesting simultaneous encapsulation of SDC molecules within dendrimer or α-CD. The distinct behavior of G5−α-CD, G5−β-CD, and G5−γ-CD on binding SDC is due to different cavity size of α-, β-, and γ-CDs. As demonstrated

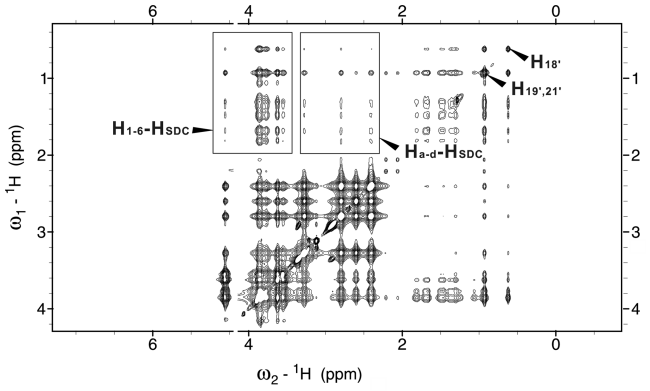

Figure 5. ^{1}H−^{1}H NOESY spectrum of SDC/G5−γ-CD complex in D_2O. The molar ratio of SDC and G5−γ-CD is 16.

before, the host ability of CDs depends on the guest/CD cavity size and guest hydrophobicity.[37] There are four aliphatic rings in the structure of SDC and the size of SDC matches better with the cavity of β/γ-CD which consists of seven or eight glucopyranose units. Therefore, G5−β/γ-CD shows higher priority to bind SDC molecules within the CD cavity, while G5−α-CD has nonselectivity in SDC encapsulation. It is worth noting that the solutions of G5−α-CD and G5−β-CD become a bit cloudy after the addition of SDC molecules and a slight decrease in SDC signals was observed in the ^{1}H NMR spectrum of the SDC/G5−CD complex solution (Figure S5 in the Supporting Information).

In the case of SMZ/G5−CD complexes, SMZ also showed simultaneous encapsulation by G5 dendrimer and CDs in the presence of the three conjugates (Figure 6 and Figure S6 in the

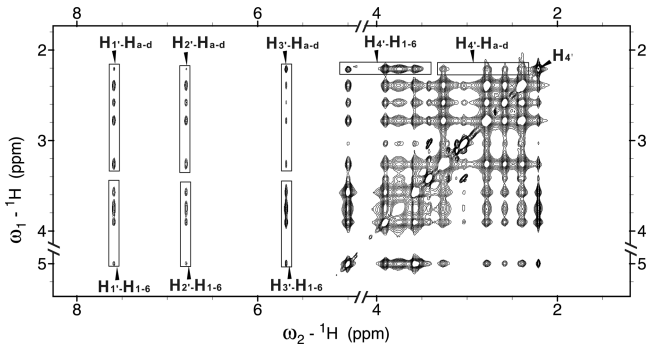

Figure 6. ^{1}H−^{1}H NOESY spectrum of the SMZ/G5−α-CD complex in D_2O. The molar ratio of SMZ and G5−α-CD is 16.

Supporting Information). SMZ is poorly soluble in aqueous solution (<0.5 mg/mL). We found that all the three conjugates significantly improved the solubility of SMZ in D_2O. Comparable intensities of NOE cross peaks for SMZ/CD and SMZ/G5 are observed for the three complexes. SMZ shows much weaker NOE cross peaks with γ-CD than with α-CD and β-CD. This is probably due to the fact that the size of SMZ is much smaller than the cavity size of γ-CD.

Figure 7 shows the NOESY spectrum of MTX/G5−α-CD complex. It is observed that MTX shows strong NOE interactions with G5 dendrimer protons and extremely low NOE interactions with α-CD protons, suggesting that MTX has higher priority to bind with G5 dendrimer rather than with α-CD. In comparison, G5−γ-CD simultaneously encapsulates MTX molecules within the CD and G5 dendrimer cavities

dx.doi.org/10.1021/jp3062916 | J. Phys. Chem. B 2012, 116, 11217−11224

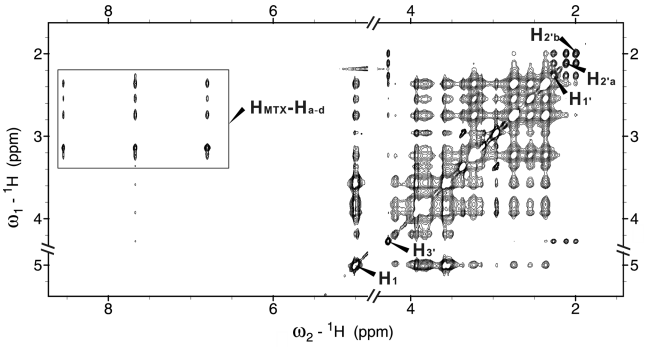

Figure 7. ^{1}H−^{1}H NOESY spectrum of the MTX/G5−α-CD complex in D_2O. The molar ratio of MTX and G5−α-CD is 16.

(Figure S7 in the Supporting Information). Like SDC, MTX with a relatively large molecular size that matches β-CD and γ-CD. Therefore, distinct encapsulation behaviors of G5−α-CD and G5−γ-CD toward MTX are obtained. Unfortunately, MTX and G5−β-CD form precipitates in their complex solution. Decreased MTX signals were observed in the ^{1}H NMR spectrum of MTX/G5−β-CD complex solution. As a result, extremely weak NOE signals can be observed in the NOESY spectrum in Figure S7b, which prevents the analysis of MTX localization within G5−β-CD. Among α-, β-, and γ-CDs, the molecular size of MTX is most matched to the cavity size of β-CD. Therefore, most of the MTX molecules are encapsulated within the β-CD on the surface of the G5 dendrimer in the MTX/G5−β-CD complex, while MTX molecules are mainly located within G5 pockets in the MTX/G5−α-CD complex, and both located in G5 pockets and γ-CD in the MTX/G5−γ-CD complex. It is reported that MTX molecules have two carboxyl groups forming cross-linking supramolecular structures with cationic PAMAM dendrimer.[13] Large numbers of MTX molecules bound on the surface of G5−β-CD may facilitate this process and result in the formation of precipitates. Therefore, only the MTX/G5−β-CD complex solution was observed with precipitates.

In all the NOESY spectra of G5−CD conjugates, we observe NOE cross peaks between dendrimer interior protons (H_a−H_d) and CD protons (H_{1-6}), suggesting that partial CD molecules conjugated on dendrimer surface are encapsulated within dendrimer pockets. For the guest molecules encapsulated within G5 dendrimer, the guest molecules are localized in deeper pockets of the G5 PAMAM dendrimer rather than in the outermost layer pockets of the dendrimer. Take SMZ and MTX for example, the presence of NOE cross peaks between SMZ/MTX protons and interior dendrimer protons (H_a−H_d, Scheme 2) and the absence of NOE cross peaks between these guest protons and dendrimer surface methylene protons ($H_{b'}$ and $H_{d'}$) were observed in Figures 6 and 7, and Figure S6 in the Supporting Information. This localization behavior is also reported in our previous studies on PAMAM dendrimer/drug complexes.[24] It is worth noting that the complexes of SDS and MTX with G5−α-CD and G5−β-CD are not stable in aqueous solutions and precipitates were observed in these complex solutions. This problem can be solved by the acetylation of residual amine groups on G5 dendrimer surface[16,17] Acetylated G5−β-CD/MTX solution was obtained without precipitate and the solution can be kept clear during a period of several weeks. The acetylation strategy can not only improve the stability and solubility of G5−CD conjugates but also increase their biocompatibility when delivering therapeutic agents.[43−45] We are now in the process of evaluating the anticancer drug loading and delivery efficiency of these acetylated G5−CD conjugates.

CONCLUSIONS

We synthesized and characterized G5 PAMAM dendrimer and α-, β-, and γ-CD conjugates. The complexes of five guest molecules with the G5−CD conjugates were prepared and analyzed by NOESY spectrum. The encapsulation of guest molecules within CDs or G5 dendrimer depends on the guest size, CD cavity size, and guest hydrophobicity. For example, ADH with a molecular size matched to β-CD cavity only binds with β-CD in the G5−β-CD conjugate (Table 2). Similarly,

Table 2. Selective Encapsulation of Five Guest Molecules within the Three G5−CD Conjugates

Selective Encapsulation Pattern	Complexes	Advantages
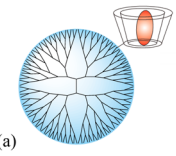 (a)	ADH/G5-α-CD ADH/G5-β-CD SDC/G5-β-CD SDC/G5-γ-CD SDS/G5-β-CD SDS/G5-γ-CD	Expanding the scope of drugs
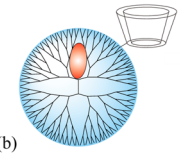 (b)	MTX/G5-α-CD	Improving solubility, biocompatibility, and cellular uptake
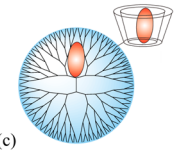 (c)	SMZ/G5-α-CD SMZ/G5-β-CD SMZ/G5-γ-CD SDC/G5-α-CD MTX/ G5-γ-CD	Improving drug loading capacity
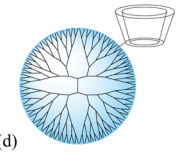 (d)	ADH/G5-γ-CD	Not applicable

SDS with a long aliphatic chain prefers to localize within the α-CD cavity, and SDC and MTX with relatively large size prefer to bind with γ-CD and β-CD in the G5−β-CD and G5−γ-CD conjugates. In the MTX/G5−α-CD complex, MTX tends to localize within the G5 dendrimer rather than within α-CD. However, in the complexes of SMZ/G5−CD and SDC/G5−α-CD, simultaneous encapsulation of SMZ/SDC within CD or G5 was observed (Table 2). The combination of PAMAM dendrimer and α-, β-, γ-CD can improve the drug loading ability of dendrimer and make more drugs suitable for dendrimer-based drug delivery systems (such as ADH). All the G5−CD conjugates can significantly improve the aqueous solubility of poorly soluble drugs such as SMZ. Though some of the complexes show poor aqueous solubility, acetylation of the G5−CD conjugate can efficiently prevent the precipitate formation. In summary, the present data on G5−CD conjugates and their derivates are useful in the design and optimization of dendrimer-based drug delivery systems. Further in vitro and in vivo biological analysis of these conjugates remains to be investigated in detail.

dx.doi.org/10.1021/jp3062916 | J. Phys. Chem. B 2012, 116, 11217−11224

■ ASSOCIATED CONTENT

Supporting Information

Further information on ^{1}H NMR and ^{1}H−^{1}H NOESY spectra of G5−CD conjugates and G5−CD/guest complexes. This material is available free of charge via the Internet at http://pubs.acs.org.

■ AUTHOR INFORMATION

Corresponding Author

*E-mail: yycheng@mail.ustc.edu.cn.

Notes

The authors declare no competing financial interest.

■ ACKNOWLEDGMENTS

We thank the Science and Technology of Shanghai Municipality (11DZ2260300), the Talent Program of East China Normal University (No. 77202201), the Program for New Century Excellent Talents in University of Ministry of Education of China, and the Innovation Program of Shanghai Municipal Education Commission (No. 12ZZ044) on this project for financial support.

■ REFERENCES

(1) Tomalia, D. A. *New J. Chem.* **2012**, *36*, 264.
(2) Tomalia, D. A. *Soft Matter* **2010**, *6*, 456.
(3) Tomalia, D. A. *Prog. Polym. Sci.* **2005**, *30*, 294.
(4) Tomalia, D. A.; Reyna, L. A.; Svenson, S. *Biochem. Soc. Trans.* **2007**, *35*, 61.
(5) Menjoge, A. R.; Kannan, R. M.; Tomalia, D. A. *Drug Discov. Today* **2010**, *15*, 171.
(6) Svenson, S.; Tomalia, D. A. *Adv. Drug Delivery Rev.* **2005**, *57*, 2106.
(7) Cheng, Y. Y.; Zhao, L. B.; Li, Y. W.; Xu, T. W. *Chem. Soc. Rev.* **2011**, *40*, 2673.
(8) Astruc, D.; Boisselier, E.; Ornelas, C. *Chem. Rev.* **2010**, *110*, 1857.
(9) Svenson, S. *Eur. J. Pharm. Biopharm.* **2009**, *71*, 445.
(10) Svenson, S.; Chauhan, A. S. *Nanomedicine* **2008**, *3*, 679.
(11) Tomalia, D. A.; Baker, H.; Dewald, J.; Hall, M. G. K.; Martin, S.; Roeck, J.; Ryder, J.; Smith, P. *Polym. J.* **1985**, *17*, 117.
(12) Zhao, L. B.; Wu, Q. L.; Cheng, Y. Y.; Zhang, J. H.; Wu, J. H.; Xu, T. W. *J. Am. Chem. Soc.* **2010**, *132*, 13182.
(13) Zhao, L. B.; Cheng, Y. Y.; Hu, J. J.; Wu, Q. L.; Xu, T. W. *J. Phys. Chem. B* **2009**, *113*, 14172.
(14) Wu, Q. L.; Cheng, Y. Y.; Hu, J. J.; Zhao, L. B.; Xu, T. W. *J. Phys. Chem. B* **2009**, *113*, 12934.
(15) Cheng, Y. Y.; Li, Y. W.; Wu, Q. L.; Xu, T. W. *J. Phys. Chem. B* **2008**, *112*, 12674.
(16) Yang, K.; Weng, L.; Cheng, Y. Y.; Zhang, H. F.; Zhang, J. H.; Wu, Q. L.; Xu, T. W. *J. Phys. Chem. B* **2011**, *115*, 2185.
(17) Fang, M.; Zhang, J.; Wu, Q. L.; Xu, T. W.; Cheng, Y. Y. *J. Phys. Chem. B* **2012**, *116*, 3075.
(18) Hu, J. J.; Cheng, Y. Y.; Wu, Q. L.; Zhao, L. B.; Xu, T. W. *J. Phys. Chem. B* **2009**, *113*, 10650.
(19) Cheng, Y. Y.; Wu, Q. L.; Li, Y. W.; Xu, T. W. *J. Phys. Chem. B* **2008**, *112*, 8884.
(20) Ortiz-Mellet, C.; García-Fernández, J. M.; Benito, J. M. *Chem. Soc. Rev.* **2011**, *40*, 1586.
(21) Zhang, J.; Ellsworth, K.; Ma, P. X. *J. Controlled Release* **2010**, *145*, 116.
(22) Bellia, F.; La Mendola, D.; Pedone, C.; Rizzarelli, E.; Saviano, M.; Vecchio, G. *Chem. Soc. Rev.* **2009**, *38*, 2756.
(23) Li, J.; Loh, X. J. *Adv. Drug Delivery Rev.* **2008**, *60*, 1000.
(24) Hu, J. J.; Cheng, Y. Y.; Ma, Y. R.; Wu, Q. L.; Xu, T. W. *J. Phys. Chem. B* **2009**, *113*, 64.
(25) Wada, K.; Arima, H.; Tsutsumi, T.; Chihara, Y.; Hattori, K.; Hirayama, F.; Uekama, K. *J. Controlled Release* **2005**, *104*, 397.
(26) Benito, J. M.; Gomez-Garcia, M.; Ortiz Mellet, C.; Baussanne, I.; Defaya, J.; Garcia Fernandez, J. M. *J. Am. Chem. Soc.* **2004**, *126*, 10355.
(27) Kihara, F.; Arima, H.; Tsutsumi, T.; Hirayama, F.; Uekama, K. *Bioconjugate Chem.* **2002**, *13*, 1211.
(28) Garnero, C.; Zoppi, A.; Genovese, D.; Longhi, M. *Carbohydr. Res.* **2010**, *345*, 2550.
(29) Arima, H.; Yamashita, S.; Mori, Y.; Hayashi, Y.; Motoyama, K.; Hattori, K.; Takeuchi, T.; Jono, H.; Ando, Y.; Hirayama, F.; et al. *J. Controlled Release* **2010**, *146*, 106.
(30) Motoyama, K.; Hayashida, K.; Higashi, T.; Arima, H. *Bioorg. Med. Chem.* **2012**, *20*, 1425.
(31) Kojima, C.; Toi, Y.; Harada, A.; Kono, K. *Bioconjugate Chem.* **2008**, *19*, 2280.
(32) Zhang, W.; Chen, Z.; Song, X.; Si, J.; Tang, G. *Technol. Cancer Res. Treat.* **2008**, *7*, 103.
(33) Hu, J. J.; Xu, T. W.; Cheng, Y. Y. *Chem. Rev.* **2012**, *112*, 3856.
(34) Brand, T.; Cabrita, E. J.; Berger, S. *Prog. Nucl. Magn. Reson. Spectrosc.* **2005**, *46*, 159.
(35) Granadero, D.; Bordello, J.; Perez-Alvite, M. J.; Novo, M.; Al-Soufi, W. *Int. J. Mol. Sci.* **2010**, *11*, 173.
(36) Zhang, J. X.; Ellsworth, K.; Ma, P. X. *J. Controlled Release* **2010**, *145*, 116.
(37) Eftuink, M. R.; Andy, M. L.; Bystrom, K.; Perlmutter, H. D.; Kristol, D. S. J. *J. Am. Chem. Soc.* **1989**, *111*, 6765.
(38) Fang, M.; Cheng, Y. Y.; Zhang, J. H.; Wu, Q. L.; Hu, J. J.; Zhao, L. B.; Xu, T. W. *J. Phys. Chem. B* **2010**, *114*, 6048.
(39) Yang, K.; Cheng, Y. Y.; Feng, X. Y.; Zhang, J. H.; Wu, Q. L.; Xu, T. W. *J. Phys. Chem. B* **2010**, *114*, 7265.
(40) Sehgal, P.; Sharma, M.; Wimmer, R.; Larsen, K. L.; Otzen, D. E. *Colloid Polym. Sci.* **2006**, *284*, 916.
(41) Qu, X. K.; Zhu, L. Y.; Li, L.; Wei, X. L.; Liu, F.; Sun, D. Z. *J. Solution Chem.* **2007**, *36*, 643.
(42) Andreaus, J.; Draxler, J.; Marr, R.; Lohner, H. *J. Colloid Interface Sci.* **1997**, *185*, 306.
(43) Waite, C. L.; Sparks, S. M.; Uhrich, K. E.; Roth, C. M. *BMC Biotechnol.* **2009**, *9*, 38.
(44) Kolhatkar, R. B.; Kitchens, K. M.; Swaan, P. W.; Ghandehari, H. *Bioconjugate Chem.* **2007**, *18*, 2054.
(45) Fant, K.; Esbjorner, E. K.; Jenkins, A.; Grossel, M. C.; Lincoln, P.; Norden, B. *Mol. Pharm.* **2010**, *7*, 1734.